Journal of Electroanalytical Chemistry 692 (2013) 31–39

Contents lists available at SciVerse ScienceDirect

Journal of Electroanalytical Chemistry

journal homepage: www.elsevier.com/locate/jelechem

Understanding electrochemical stability of Cu^+ on zeolite modified electrode with Cu-ZSM5

M.A. Oliver-Tolentino [a,b], A. Guzmán-Vargas [a,*], E.M. Arce-Estrada [c], D. Ramírez-Rosales [d], A. Manzo-Robledo [e], E. Lima [f]

[a] ESIQIE-IPN, Departamento de Ingeniería Química, Laboratorio de Investigación en Materiales Porosos, Catálisis Ambiental y Química Fina, UPALM Edif. 7 P.B. Zacatenco, GAM, México, DF 07738, Mexico
[b] UPIBI-IPN, Departamento de Ciencias Básicas, Av. Acueducto s/n, Barrio La Laguna, Col. Ticomán, GAM, México, DF 07340, Mexico
[c] ESIQIE-IPN, Departamento de Ingeniería en Metalurgia y Materiales, UPALM Edif. 7 P.B. Zacatenco, GAM, México, DF 07738, Mexico
[d] ESFM-IPN, Departamento de Física, UPALM Edif.9 Zacatenco, GAM, México, DF 07738, Mexico
[e] ESIQIE-IPN, Departamento de Ingeniería Química, Laboratorio de Electroquímica y Corrosión, Edif. Z-5 3er piso, UPALM, Zacatenco, GAM, México, DF 07738, Mexico
[f] IIM-UNAM, Circuito Exterior s/n, Cd. Universitaria, Del. Coyoacán, México, DF 04510, Mexico

ARTICLE INFO

Article history:
Received 26 April 2012
Received in revised form 15 December 2012
Accepted 21 December 2012
Available online 5 January 2013

Keywords:
ZME
Cu-ZSM5
Electroreduction
Redox couple
Cyclic voltammetry

ABSTRACT

In the present work the system Cu-ZSM5 was prepared by aqueous ion-exchange method from zeolite H-ZSM5. The solids were characterized by X-ray diffraction, nitrogen physisorption, temperature-programmed reduction with hydrogen (TPR-H_2) and electron paramagnetic resonance (EPR). These porous materials were mixed with poly (methacrylic acid methyl ester) and methyl acrylate (MA), and immobilized on a glassy carbon electrode in order to obtain the so-called zeolite-modified electrode (ZME). The as-prepared electrodes were characterized by infrared spectroscopy and electrochemical techniques as cyclic voltammetry and chronocoulometry. The presence of copper in the zeolite was confirmed by TPR-H_2. The XRD results indicate not important structural changes in the zeolite ZSM5 due to copper incorporation. The EPR spectroscopy showed that copper in Cu-ZSM5 is as isolated form of Cu^{2+} ions. The results of nitrogen physisorption suggest that the Cu^{2+} cations are occupying the exchange sites in zeolite ZSM5. On the other hand, the IR spectroscopy revealed the presence of C=O and C=C groups in the mixture Cu-zeolite/polymer. The electrochemical profiles showed that reduction of Cu^{2+} to Cu^0 occurs by two steps in presence of chloride due to stabilization of Cu^+. The influence of anion in the electrolyte suggests that the redox processes Cu^{2+} to Cu^+ and Cu^+ to Cu^0 occurs on the zeolite-modified electrode even at nitrate- and sulfate-based solutions at the glassy carbon/zeolite interface. This stabilization is mainly associated to the interactions between Cu^+ and C=C group and the zeolite framework acting as "electron reservoir".

1. Introduction

Zeolite-modified electrodes (ZMEs) have attracted considerable attention during the past years because they combine, in a single device, the specificity of charge transfer reactions with the intrinsic properties of the aluminosilicates, such as molecular sieving and ion exchange capacity [1–4]. In the electrochemical fields the zeolites have been used in electrocatalysis and in electrochemical sensors [5–9]. However a critical point in applying ZMEs in this area is their preparation. Zeolites are insulating materials; therefore, their use in electrochemical systems requires a close contact with an electronically conducting support. In this context, zeolite immobilization in the supporting material are often reported (i) zeolite modified carbon paste electrodes (ZMCPEs), where zeolite particles are dispersed within a mixture of graphite powder and mineral oil binder [10]; (ii) binder free ZMEs based on dry graphite zeolite mixtures pressed on a stainless steel grid [11]; and (iii) zeolite polymer films coated on solid electrode surfaces, where the polymer acts as a binder to stick together the zeolite particles [12]. The most intriguing question arising when considering the electrochemical response of redox probes confined in ZMEs is how electrons can be transferred to/from these guest species from/to the electrode surface (i.e., the conducting part of the ZME). Among all observations and discussions that have appeared in the literature, one can now distinguish three mechanisms: (1) extra zeolite electron transfer, (2) intrazeolite electron transfer and (3) electron transfer to/from species located at the outermost boundaries of the zeolite particles. In the extrazeolite electron-transfer mechanism, the redox species are first ion-exchanged by

* Corresponding author. Tel.: +57 296000x55163.
E-mail address: aguzmanv@ipn.mx (A. Guzmán-Vargas).

1572-6657/$ - see front matter © 2013 Elsevier B.V. All rights reserved.
http://dx.doi.org/10.1016/j.jelechem.2012.12.015

the electrolyte cations and then diffuse to a conducting part of the electrode surface to undergo charge transfer. In the intrazeolite electron-transfer mechanism, charge transfer occurs via electron hopping between adjacent redox species located in the zeolite structure. Whereas in the case of "boundary associated" species, also called "topological redox isomers", the electrons transfer processes involve species that are attached to the zeolite surface (or occluded in cages located at the outermost surface of the zeolite particle) and not likely to be desorbed prior to charge transfer.

The most studied zeolites have been FAU and LTA. Recently, some reports have been published about the electrochemical behavior of ZMEs prepared with ZSM5 [13–18]. Zeolite Sieve of Molecular porosity-5 (MFI or ZSM5) is an aluminosilicate belonging to the pentasil family of zeolites composed of several units linked together by oxygen bridges to form pentasil chains. A pentasil unit consists of eight five-membered rings. In these rings, the vertices are Al or Si, where the O is bonded between the vertices. The estimated pore size of the channel running parallel with the corrugations is 5.4–5.6 Å [19]. This zeolite can be prepared with high Si/Al ratio. Due to differences between Al^{3+} and Si^{4+} cation valances, the presence of tetrahedrally coordinated Al in the zeolite framework creates an anionic site that must be charge compensated with a cation. In the acidic form of the zeolite, the cation in turn is a proton (H^+). Thus, the acidity is proportional to the Al content. The regular 3D channel structure and the acid properties of H-ZSM5 can be appropriated for acid-catalyzed reactions such as synthetic gasoline production, isomerization, cracking and reforming [20]. Additionally, in recent years, modified zeolites have attracted attention for their performance in many other applications. For instance, zeolite-containing transition metal ions showed high activities for several reactions. For example, the Cu-ZSM5 has been used in some reactions such as selective catalytic reduction of nitrogen oxides (SCR-NO_x) [21,22], oxidation of benzene to phenol [23,24] and methane to methanol [25]. The catalytic activity has been associated to the nature of copper sites and their redox chemistry inside the zeolite structure, induced by the high energy of the Cu(I)-HOMO orbital at ZSM5 and to the π back-electron donation from the Cu-*d* orbitals to π^*-antibonding orbitals [26,27].

On the other hand, intra and extra zeolitic mechanisms have been proposed in order to understand the electrochemical role of copper inside Y-, A- and Mordenite-type zeolites [28]. Furthermore, Li and Calzaferri proposed a third mechanism called intrazeolite ion transport for electrode process [29]. According to this, in nitrate-based solution, the cupric ions inside the zeolite are reduced directly to their metallic states due to the reduction of Cu^{2+} via a single two-electron step. However, in complex forming substances, as in the case of chloride-ions based solutions, the electrochemical reduction of Cu^{2+} occurs in two steps with one-to-one electron transfer due to formation of $CuCl_2^-$ [30,31].

In this work is proposed a new way for the immobilization of Cu-ZSM5 using poly (methacrylic acid methyl ester) and methyl acrylate (MA). The study is mainly focused on the influence of the substrate, supporting electrolyte, electrode preparation procedure and thermal treatment over the interfacial electrochemistry.

2. Experimental section

2.1. Cu-ZSM5 preparation

The parent zeolite was NH_4-ZSM5 (from Zeolyst CBV3024E, Si/Al = 15, S_{BET} = 400 $m^2\ g^{-1}$). H-ZSM5 form was obtained by calcination of parent zeolite in air at 773 K/5 h. The Cu-ZSM5 was prepared by ion-exchange method and labeled Cu(*x*)-ZSM5, *x* being the theoretical exchange degree (*x* = 200 × Cu/Al, mol/mol). Briefly, 2 g of H-ZSM5 was added to 500 cm^3 of $Cu(NO_3)_2\ 7H_2O$ aqueous solution and stirred for 48 h at room temperature. Then, the solid was filtered, washed three times with de-ionized water and dried at 353 K in air atmosphere. The resulting solid was calcined at 773 K in air for 8 h (50 $cm^3\ min^{-1}$, ramp: 10 K min^{-1}).

2.2. Working electrode preparation

A polymer solution was obtained using 3 mg of poly-methacrylic acid methyl ester, PMMA, (Aldrich, USA) dissolved in 1 mL of methyl acrylate, MA, (Aldrich, USA). The solution was mixed with 0.2 g of Cu-ZSM5 or H-ZSM5. The mixture was homogeneously dispersed in ultrasound for 30 min. Then, 0.5 μL of the resulting suspension was deposited at the surface of glassy carbon electrode (4 mm diameter) and dried with argon at room temperature. The obtained zeolite-modified electrodes (ZME) were labeled as ME/Cu-ZSM5 and ME/H-ZSM5.

2.3. Electrochemical measurements

The electrochemical analyses were carried out at room temperature in a potentiostate–galvanostate VERSASTAT3-400 (Princeton Applied Research). A three-electrode standard electrochemical cell was used for the cyclic voltammetry (CV) measurements at 20 mV s^{-1}. A carbon rod and a Calomel (SCE) electrode were used as counter and reference electrode, respectively. Prior to use, the solution was purged with argon for at least 15 min. The *i-E* characteristics were recorded in the interval from −0.5 V to 0.5 V/SCE. The initial potential was fixed at open-circuit potential toward cathodic direction. Solutions 0.1 M of NaCl, $NaNO_3$, and 0.05 M Na_2SO_4 were used as supporting electrolyte.

2.4. XRD, TPR-H_2, BET, IR and EPR spectra analysis

XRD patterns of the samples, as prepared or calcined at 773 K, were recorded on a D8 Focus Bruker AXS instrument using Cu-Kα1 radiation (λ = 1.542 Å, 35 kV, and 25 mA). TPR-H_2 analysis was carried out with a Micromeritics AutoChem 2910 apparatus using TCD detection. The TPR was carried out with H_2/Ar (25/75, v/v) after calcination of 200 mg sample at 823 K in air for 2 h, then cooled to room temperature (RT) in air. After outflowing the sample with air, the TPR is then started up to 1300 K (flow: 13 cm^3 - min^{-1}; ramp:10 K min^{-1}). N_2 sorption experiments at 77 K were carried out on samples previously calcined at 723 K and outgassed at 553 K (10–4 Pa), with a Micromeritics ASAP 2000 instrument. Specific surface areas were calculated using the BET method. Absorption/transmission IR spectra were run using a Perkin Elmer RX-1 spectrophotometer with attenuated total reflectance accessory (ATR), working in the range from 4000 to 400 cm^{-1} at a resolution of 4 cm^{-1} (number of scans 64). CW EPR (continuous wave EPR) spectra were acquired using a JEOL JES-RES3X ESR spectrometer equipped with a PC for spectrometer control and data acquisition. Typical EPR spectral parameters were the following: X-band frequency = 9.1642 GHz, modulation amplitude = 3.2 G, modulation frequency = 100 kHz. The magnetic field and microwave frequency were measured using a Hall probe and a frequency counter, respectively. Quantification of Cu^{2+} from Cu-ZSM5 sample was performed by obtaining the double integral of the 1st derivative curve of the EPR spectrum of $CuSO_4{\cdot}5H_2O$ standard using identical EPR parameters.

3. Results and discussion

3.1. XRD patterns

In Fig. 1A the XRD patterns for sample Cu-ZSM5 and H-ZSM5 are compared. The pattern corresponding to Cu-ZSM5 not showed important differences respect to H-ZSM5 pattern. Moreover, in particular two regions are delimited, $2\theta = 24°–20°$ (Fig. 1B) and 34°–40° (Fig. 1C), in the first region there is a small shift in the peaks at 23°, 27° and 29.5° 2θ associated to the presence of Cu species from the cationic exchange fairly than a loss of structure, this fact and the absent of the peaks in the second region ($2\theta = 34–40$) at 2θ 35.55° and 38.73° which could be attributed to the CuO as secondary phase [32], indicate a highly and uniform dispersion of Cu-ions in compensating positions inside the zeolite.

3.2. TPR-H_2 profile and adsorption isotherm

Temperature-programmed reduction (TPR) of Cu-ZSM5 was carried out in order to obtain additional information about the oxidation state of copper and discard the presence of CuO into the zeolite. The TPR-H_2 profile of Cu-ZSM5 material (Figure not shown) exhibits one peak c.a. 453 K is attributable to the reduction of Cu^{2+} to Cu^{+} and Cu^{+} to Cu^{0}. Any evidence of the CuO reduction was observed around 700 K as has been reported in ref [33], keeping mind that the preparation method and analysis conditions (ramp temperature, flow and hydrogen concentration) have influence on TPR-H_2 results. Cu-ZSM showed typical type-1 isotherm, according to IUPAC classification; the H-ZSM5 zeolite parent exhibited the same isotherm (not shown). From BET analysis, the calculated area was 400 $cm^2\ g^{-1}$ for both samples. These results confirm that copper species are located in exchange position on the channel zeolite structure [34].

3.3. IR–ATR spectra

Remaining of polymer and solvent (PMMA and MA) in the Cu-ZSM5 mixture was investigated by IR spectroscopy. The IR–ATR spectrum for the Cu-ZSM5 (curve a), mixture Cu-ZSM5/MA (curve b), and mixture Cu-ZSM5/PMMA/MA (curve c) dried with argon at room temperature are shown in Fig. 2. In all cases, the characteristic bands of zeolite ZSM5 in the range of 500–1300 cm^{-1} are observed. The band at c.a. 799 cm^{-1} corresponds to internal- and external-symmetrical vibrations of the structure Si–O–Si [35]. The band around 1070 cm^{-1} is attributed to the internal-asymmetric stretching vibration of Si–O–T [36]. Whereas, the external-asymmetric stretching vibration near 1220 cm^{-1} is due to the presence of structures containing four chains of five-membered rings arranged around a twofold screw axis, as in the case of ZSM-5 structure. The bands at c.a. 1625 cm^{-1} and 2400 cm^{-1} are associated to physisorbed water in the zeolite framework [37]. On the other hand, at 1713 cm^{-1} a band attributed to carbonyl group (C = O) can be observed, this vibration is due to the presence of PMMA and MA, which contain this functional group [38]. The band at c.a. 1625 cm^{-1} is characteristic of C = C interaction, suggesting that MA is present in the mixture even when the sample was dried.

3.4. Electron paramagnetic resonance analysis

Prior to electrode preparation, the EPR spectroscopy was used to identify copper species. Spectra of Cu-ZSM5 (curve a) and Cu-ZSM5/MA mixture (curve b) are presented in Fig. 3. Each sample was cooled at 77 K for data acquisition to eliminate the effects of motional broadening which are apparent at room temperature (not shown). The EPR spectra of Cu-ZSM5 and Cu-ZSM5/MA samples at 77 K are characterized by axial anisotropy of the g factor with a resolved hyperfine structure due to isolated Cu^{2+} species. Each spectrum exhibits four hyperfine features ($m_I = -3/2, -1/2, +1/2, +3/2$) in the low field region of the spectrum, characteristic of the copper nucleus with $I = 3/2$. Although the EPR spectra in Fig. 3 are qualitatively similar, there are subtle differences in the positions of the low field hyperfine. A spectral broadening in sample Cu-ZSM5/MA increases. This broadening is observed in the EPR spectrum of curve (b) and can be attributed to correlated g and A strain. Strain results from the heterogeneity in the micro-environments of the paramagnetic center (Cu^{2+}) that lead to a distribution of g and A values [39]. Heterogeneity in the micro-environments of the Cu^{2+} sites, suggest that the distortion involved the displacement of copper along the parallel axis resulting in a reduction of the symmetry from D_{4h} to C_{2V} [40]. The EPR parameters ($g_{\|} = 2.36, g_{\perp} = 2.07, A_{\|} = 140\ G$) indicate that these spectra are caused by Cu^{2+} ions stabilized in octahedral crystal fields induced by oxide ligands. These findings are consistent with numerous data for EPR spectra of Cu^{2+} ions in hydrated zeolites of different types [41,42].

The EPR parameters of extant Cu^{2+} ions in the Cu-ZSM5/MA mixture correspond to an octahedral copper coordination with a

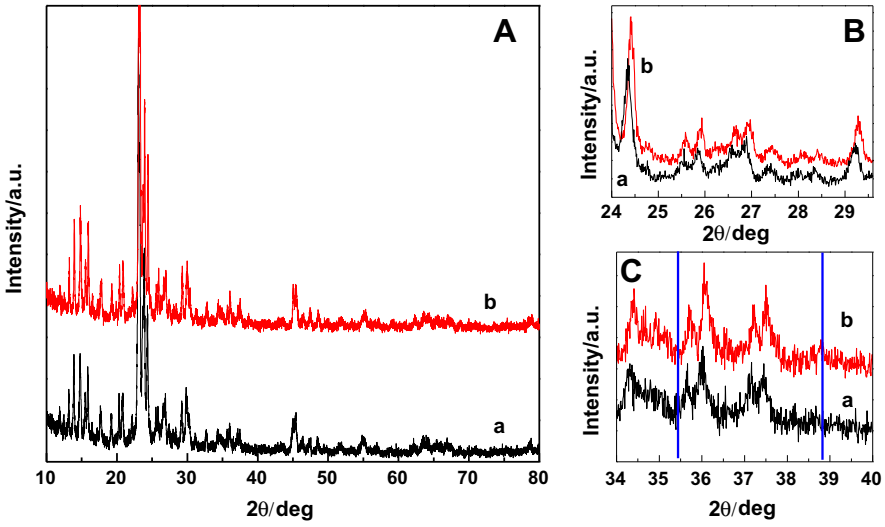

Fig. 1. X-ray diffraction patterns (A) of samples (a) parent zeolite HZSM5, (b) Cu-ZSM5; Inset: detailed XRD patterns for the sample ranged from (B) 24–30 and (C) 34–40 $2\theta°$, the blue dashed lines point out the absent of the characteristic peaks position of CuO. The peaks were indexed according to JCPDS card No. 5-0661.

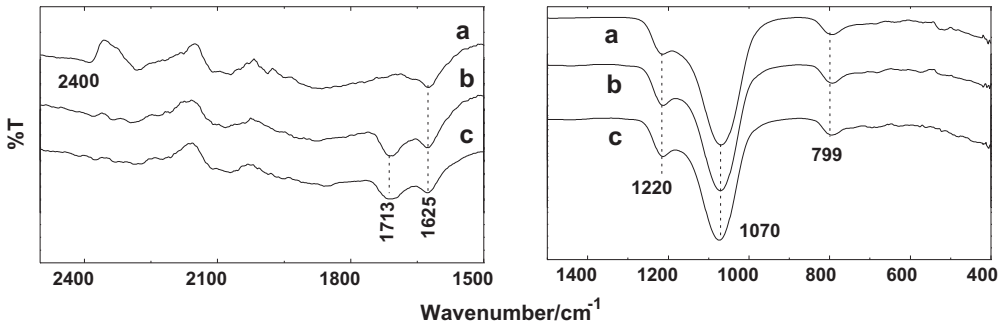

Fig. 2. IR–ATR spectra of (a) Cu-ZSM5, (b) Cu-ZSM5/MA and (c) Cu-ZSM5/PMMA/MA.

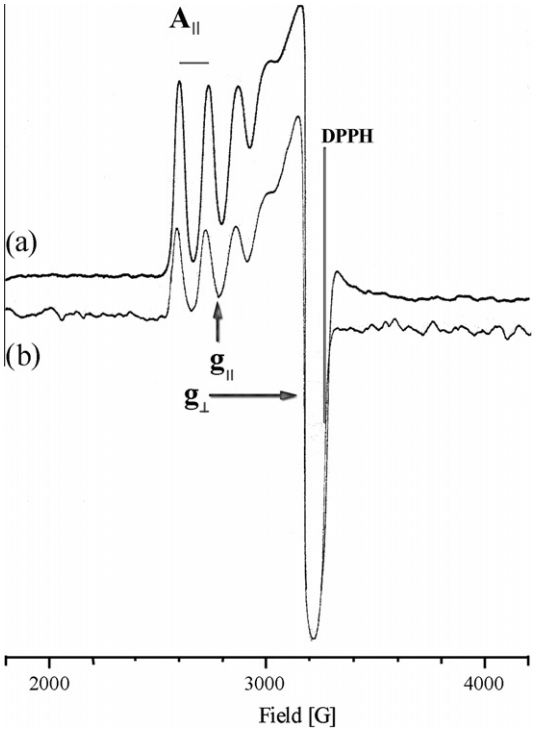

Fig. 3. EPR spectra of (a) Cu-ZSM5, (b) Cu-ZSM5/MA at 77 K.

tetragonal distortion. The degree of tetragonal distortion for some ions ($g_{\|} = 2.37, g_{\perp} = 2.07, A_{\|} = 143\ G$) is noticeable, which calls for special analysis of the nature of ligands that provide highly covalent bonds to copper.

The EPR spectrum of Cu-ZSM5/MA sample recorded at 77 K did not show a superposition of two or more anisotropic spectra of Cu^{2+} ions and there was no background of others spectra, which would be assigned to different Cu^{2+} species like chain structures in zeolite channels [41,42]. Therefore we can assure that there is only one copper species (isolated Cu^{2+}) in both samples. The slight difference between the spectra is due to the degree of tetragonal distortion for some ions. On the other hand, from the EPR experiments the calculated content of copper exchanged on the zeolite was 0.021 %wt.

3.5. Electrochemical measurement

3.5.1. Voltammetric behavior of copper in chloride solution

The electrochemical behavior of the as-prepared Cu-ZSM5 materials was first studied in NaCl 0.1 M solution in order to establish the potential range and, in a first approach, the stability of this material. Fig. 4 shows the cyclic voltammetry (CV) profile for ME/Cu-ZSM5 (curve d). This profile has been compared with ME/H-ZSM5 (curve c), unmodified mirror finished glassy carbon (UGC, curve a) and GC covered by a thin film of PMMA (mimicking the preparation as for the Cu- and H-ZSM5, curve (b)). The potential scan, at 20 mV s^{-1}, started at open-circuit potential (OCP) in the cathodic direction. *i-E* characteristics of curves a, b and c are similar for the three electrodes, where the presence of a small contribution of non-faradic current is evident and can be associated to the double layer-charge interactions. On the other hand, in the profile corresponding to ME/Cu-ZSM5 two cathodic peaks, C_I (c.a. 0.056 V/SCE) and C_{II} (c.a. −0.351 V/SCE) and two anodic peaks, A_I (0.141 V/SCE) and A_{II} (−0.146 V/SCE) associated to oxidation reaction in the positive going scan, can be observed; being a typical behavior for this system, according to previous studies carried out by our group [43].

Necessary studies to observe the faradic process of copper were firstly carried out. Experiments at different switching potential, using a solutions of 0.1 M NaCl + 0.0005 M $CuCl_2$, were performed on UGC (curve a) and ME/H-ZSM5 (curve b) electrodes, whereas in the ME/Cu-ZSM5 (curve c) the supporting electrolyte was a solution of 0.1 M NaCl (Fig. 5). The scan was initiated from the open-circuit (E_{OCP}) in the negative direction and inverted at different potentials (E_λ), the experiments were carried out in continuous way, the electrodes were not removed from the electrolyte during the experiments for each E_λ.

All electrodes exhibit two cathodic and anodic peaks associated to copper-redox processes as represented by the following equations:

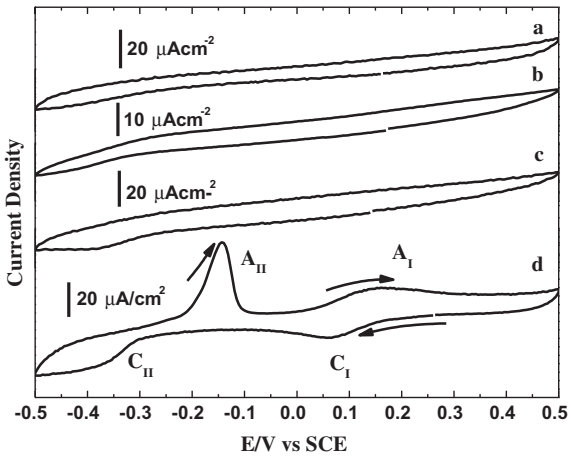

Fig. 4. *i-E* characteristics in a solution of 0.1 M NaCl for (a) UGC, (b) PMMA, (c) ME/H-ZSM5, and (d) ME/Cu-ZSM5. Scan rate 20 mV s^{-1}.

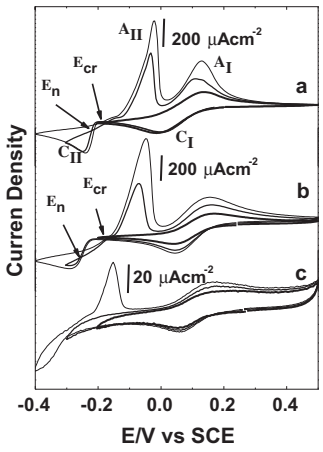

Fig. 5. Cyclic voltammetry at different switching potentials in (a) and (b) $CuCl_2$ (0.0005 M) + NaCl (0.1 M) over (a) UGC, (b) ME/H-ZSM5 electrodes, (c) in NaCl (0.1 M) over ME/Cu-ZSM5. Scan rate 20 mV s^{-1}.

Table 1
Peaks potential of electrodes in chloride solution.

	E/V vs *SCE*		
Peak	UGC	ME/H-ZSM5	ME/Cu-ZSM5
C_I	−0.004	0.045	0.057
C_{II}	−0.244	−0.275	−0.345
A_I	0.131	0.153	0.161
A_{II}	−0.019	−0.046	−0.151

$$Cu^{2+} + e^- \leftrightarrow Cu^+ \quad \text{peaks } C_I \text{ and } A_I$$

$$Cu^+ + e^- \leftrightarrow Cu^0 \quad \text{peak } C_{II} \text{ and } A_{II}$$

However, the peak-potential and current magnitude involved is different (Table 1). At E_λ = −0.2 V/SCE the *i-E* profile of UGC (curve a) showed only the presence of peaks C_I and A_I. The redox couple A_I/C_I exhibited a ΔE = 0.135 V/SCE and a formal potential (E^0 = 0.061 V/SCE), while at E_λ = −0.3 and −0.4 V/SCE the presence of peaks C_{II} and A_{II} is noticeable. The faradic processes observed in the UGC are associated to typical reduction of Cu^{2+} in presence of chloride, where the reduction of Cu^{2+} takes place via two one-electron steps due to the formation of the complex $CuCl_2^-$ (peak C_I), which promotes the Cu^+ ion stabilization in aqueous media, followed by the reduction of this complex to Cu^0 (peak C_{II}) [31]. In addition, during the positive potential sweep the oxidation of Cu^0 to Cu^+ (peak A_{II}) and Cu^+ to Cu^{2+} (peak A_I) is evident. On the other hand, two over crosses are observed. The first is known as the cross potential (E_{cr} = −0.18 V/SCE) and the second as the nucleation potential (E_n = −0.21 V/SCE). This behavior is well known [44] and it is associated to a typical response of an electro-crystallization process on a foreign substrate. This phenomenon is due to initial formation of metallic copper on UGC, when the potential scan is applied in the forward direction; upon switching the scan direction, electrodeposition takes place on the already formed copper nuclei resulting in a greater current.

For the ME/H-ZSM5 (curve b) the same electrochemical behavior that UGC can be observed, however the peaks C_I and A_I shift toward positive values, and the peaks C_{II} and A_{II} shift toward negative values (Table 1). The ΔE and E^0 between redox couple A_I/C_I was 0.108 V/SCE and 0.106 V/SCE respectively. These results suggest that (i) the Cu^+ stabilization-mechanism is different for ME/H-ZSM5 with respect to UGC and (ii) the formation of metallic copper occurs over uncovered part of glassy carbon due to the fact that the electrolyte solution permeates through the PMMA in the aperture between zeolite particles. This explanation is based on the representation of polymer–zeolite composite coatings obtained by evaporation of zeolite–polymer suspensions. Thus, in this modified electrodes two different areas can be discerning: the contact and uncovered areas. The contact area is the surface of the substrate electrode and the zeolite particles in contact each other. Whereas, the uncovered area is the free space on the substrate electrode after solvent evaporation [29].

In contrast, in the electrochemical behavior of ME/Cu-ZSM5 (curve c), the redox couple interaction A_I/C_I appear at E_λ = −0.2 and −0.3 V/SCE with a ΔE = 0.104 V/SCE and E^0 = 0.107 V/SCE. However, the peak A_{II} is only evident at E_λ = −0.4 V/SCE. Conversely, the peaks C_I and A_I shift towards more anodic potentials with respect to ME/H-ZSM5 and UGC (Table 1) electrodes. The peak C_{II} is not well defined, although the presence of peak A_{II} indicates that process C_{II} occurs at the ME/Cu-ZSM5 interface. This redox couple (A_{II}/C_{II}) shifts towards more cathodic values, no over crosses was detected. These phenomena suggest that the electrochemical reduction of Cu^{2+} in the ME/Cu-ZSM5 take place in the contact area instead uncovered part of glassy carbon. Otherwise the electrochemical behavior for Cu^{2+} in solution (ME/H-ZSM5) and Cu^{2+} inside of zeolite (ME/Cu-ZSM5) should be the same. The results discussed indicated that the charge transfer at ME/Cu-ZSM5 occurs via extrazeolitic electron-transfer mechanism as proposed by Murr et al. [45] where, at the concentration of supporting electrolyte (0.1 M), the insertion of either anion (as chloride) into the zeolite pore is not possible [46]. In this pathway, the cation in turn (in this case Na^+) acts as a charge balancing extraframework ion, gaining access into the zeolite structure with the purpose to maintain charge equilibrium [47]. The ΔE and E^0 values in chloride solution indicate that the faradic phenomena in the redox couple Cu^{2+}/Cu^+ in the ZMEs are the same, however, surprisingly, the value for the same redox couple in solution appears to be lower than for copper in the ZMEs, this can be associated to a probable behavior of these modified electrodes as a polymer gel electrolytes, where there is a highly reversible redox behavior [48], nevertheless more and different experimental studies are necessary to understand this singularity.

With the aim to observe the electrochemical behavior of ZMEs obtained by zeolite particle multilayers covered with a polymer film, ZMEs were made by this immobilization method. The sample was prepared as follow: A suspension containing 0.2 g of Cu-ZSM5 and 1 mL of methyl acrylate in a vial with a polyethylene stopper was prepared by shaking vigorously and dispersing ultrasonically for about 15 min, then, 3 μL of this dispersion was carefully applied on the surface of glassy carbon electrode and dried. After that, 3 μL of PMMA solution (3 mg of PMMA in 1 mL of methyl acrylate) were added on the dried zeolite layer; this solution was then evaporated at room temperature, the ZMEs were labeled as ME/Cu-ZSM5/PMMA. The electrochemical responses to different E_λ are exhibited in Fig. 6. The profiles at E_λ = −0.2 V and −0.3 V/SCE showed only the reduction peak (C_I) c.a. 0.039 V/SCE and an oxidation peak c.a. 0.153 V/SCE with a ΔE = 0.114 V/SCE and E^0 = 0.096 V/SCE, whereas to the E_λ = −0.4 V/SCE the peak C_{II} is not evident, but appears the peak A_{II} c.a. −0.179 V/SCE associate to the oxidation of Cu^0 to Cu^+, indicating that at E_λ = −0.4 V/SCE the metallic copper is formed during the cathodic scan. The inset presents the cyclic voltammetry at E_λ = −0.4 V/SCE of ME/Cu-ZSM5/PMMA (curve b) compared with ME/Cu-ZSM5 (curve a), it is evident that the faradic processes associated to the redox couple Cu^{2+}/Cu^+ are similar, this fact verifies that the electrochemical processes occur in the contact area as was discuss before, on the other hand, the profiles of redox couple Cu^+/Cu^0 are different, this behavior can be associated to the electrode preparation, this suggests that, for ME/Cu-ZSM5/PMMA (curve b), which was obtained by zeolite particles multilayer

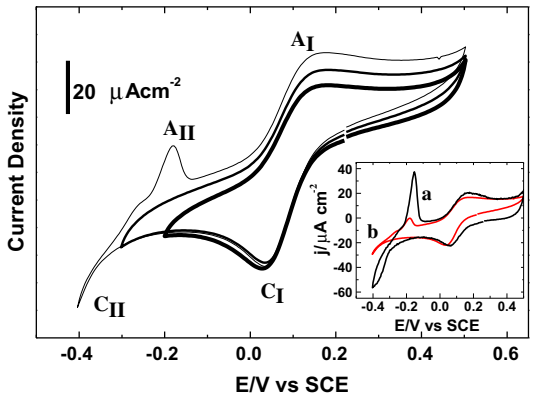

Fig. 6. Cyclic voltammetry at different switching potentials in NaCl (0.1 M) over ME/Cu-ZSM5/PMMA. Scan rate 20 mV s^{-1}, inset: comparison between (a) ME/Cu-ZSM5 (curve *c* in Fig. 5) and (b) ME/Cu-ZSM5/PMMA (Fig. 6) to E_λ = 0.4 V/SCE.

covered with a polymer film, the cation in the electrolyte solutions permeates more slowly than in the ME/Cu-ZSM5 (curve a) which was prepared by polymer–zeolite composite coatings obtained by evaporation of zeolite–polymer suspensions.

3.5.2. Chronocoulometry studies

The potential step experiments, such as chronocoulometry, can give important information about the surface state. The *Q-t* profiles obtained from ME/Cu-ZSM5 in NaCl (0.1 M) at constant potential of −0.2 V/SCE are presented in Fig. 7. The Fig. 7A exhibited the chronocoulometry of GC without Cu-ZSM5 (curve a) and of ME/Cu-ZSM5 containing different amounts of zeolite Cu-ZSM5 on the electrode surface 0.1, 0.2, 0.3, 0.5 and 0.6 mg (curves b–f, respectively). It is interesting to observe that the charge increases as a function of zeolite content. The chronocoulometric response curves of GC without Cu-ZSM5 (curve a) and ME/Cu-ZSM5 containing 0.6 mg of Cu-ZSM5 are converted to Anson plots by plotting *Q* vs $t^{1/2}$ (Fig. 7B). From this, the slope represents the charge associated to diffusion species (Q_{diff}), whereas the intercept is determined by the time-independent contributions; that is, the sum of charging of double layer (Q_{dl}) and charge associated to adsorbed species (Q_{ads}) [49]. Therefore, Q_{ads} (Fig. 7B, curve b) can be calculated by subtracting Q_{dl} (Fig. 7B, curve a) from the intercept, the Q_{diff} not change when the amount of Cu-ZSM5 is increased, this behavior suggest that the diffusion of copper ion at the interface of ME/Cu-ZSM5 is the same, regardless of the amount of Cu-Zeolite deposited on the electrode surface. The relationship between Q_{ads}–Q_{dl} and amount of Cu-ZSM5 is showed in the Fig. 7C, curve a. The Q_{ads}–Q_{dl} increases when the amount of Cu-ZSM5 increases from 0.1 to 0.3 mg and remain constant for 0.5 and 0.6 mg. This observation indicates that only the Cu^{2+} ions within the zeolite particles which are in direct contact with the surface of the glassy carbon electrode take part in the electrode process. The Cu^{2+} ions within the zeolite particles which do not directly contact the surface of the glassy carbon electrode are electrochemically 'silent', because otherwise the measured charges would be directly proportional to the amount of Cu-ZSM5 on the electrode. The Fig. 7C, curve b; showed the adsorbed amount of Cu^{2+} involved in the reduction process, this value was calculated from $Q = nF\,\Gamma_C u^{2+}$, where *Q* is the charge (Q_{ads}–Q_{dl}), *n* is the electron number, in this case *n* = 1, *F* is the faraday constant 96,480 c mol^{-1} and $\Gamma_C u^{2+}$ is the adsorbed amount of Cu^{2+}, it is clear that the quantity of copper calculated is less than the theoretical quantity of copper obtained by EPR, this result permits verify that only the Cu^{2+} located at the contact area take part in the faradic process, also this result suggests that whereas the amount of Cu-ZSM5 deposited on the electrode increases, there will be more contact area sites, where redox processes occur, this can indicate that the optimum amount of Cu-ZSM5 deposited is around of 0.7 mg. It is important to note that a greater amount of Cu-ZSM5 on the electrode produces an electrode exhibiting a poor mechanical stability.

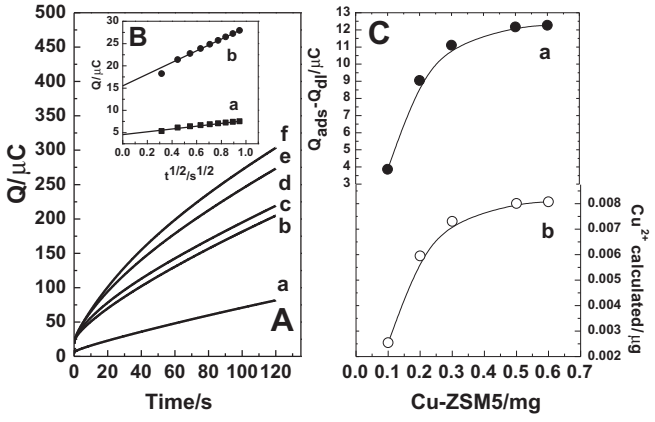

Fig. 7. Chronocoulometry studies (A) *Q* vs time to different amount of Cu-ZSM5 in the ME/Cu-ZSM5 (a) without Cu-ZSM5, (b) 0.1 mg, (c) 0.2 mg, (d) 0.3 mg, (e) 0.5 mg and (f) 0.6 mg. (B) *Q* vs $t^{1/2}$ plot (a) without Cu-ZSM5 (b) with 0.6 mg of Cu-ZSM5 and (C) Charge vs amount of Cu-ZSM5 (a) Charge and (b) Cu^{2+} calculated, the experiment was carried out in NaCl (0.1 M) the applied potential was -0.2 V/SCE.

3.5.3. Voltammetric behavior of ME/Cu-ZSM5 in solutions containing different anion

It is well known that reduction of copper ions in presence of nitrates or sulfates proceeds via a single two-electron step on ZME. Convenience experiments using different sodium based solutions containing different anion (Cl^-, NO_3^- and SO_4^{2-}) as supporting electrolyte were carried out. The *i-E* characteristics of ME/Cu-ZSM5 are exhibited in Fig. 8. The behavior in presence of chlorides (curve a) present the redox processes discussed previously. In contrast, interesting results using nitrates (curves b) and sulfates (curves c) were obtained in this study. The electrochemical profiles of ME/Cu-ZSM5 in NO_3^- revealed the presence of two reduction processes, C_I' and $C_I I'$ at 0.013 V/SCE and −0.3 V/SCE respectively, and two oxidation peaks A_I' (c.a. 0.11 V/SCE) and $A_I I'$ (c.a. −0.05 V/SCE). Whereas in presence of SO_4^{2-} the peaks C_I', A_I' and $A_I I'$ at the same potential is clearly observed. This fact can be associated to (i) reduction of Cu^{2+} by two sequential one-electron step, evidencing the Cu^+ ion stability in presence of non-chloride

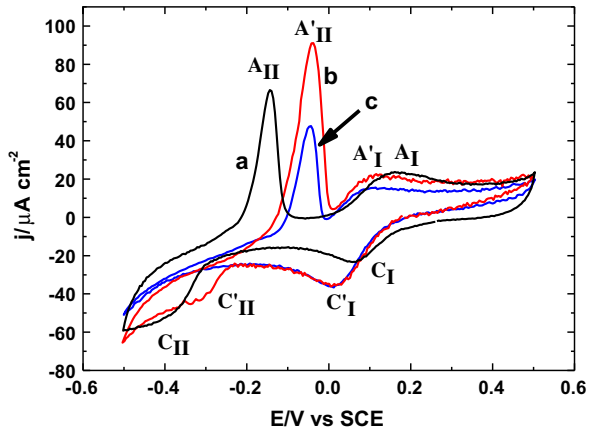

Fig. 8. Cyclic voltammetry of ME/Cu-ZSM5 in (a) NaCl (0.1 M), (b) $NaNO_3$ (0.1 M) and (c) Na_2SO_4 (0.05 M). Scan rate 20 mV s^{-1}.

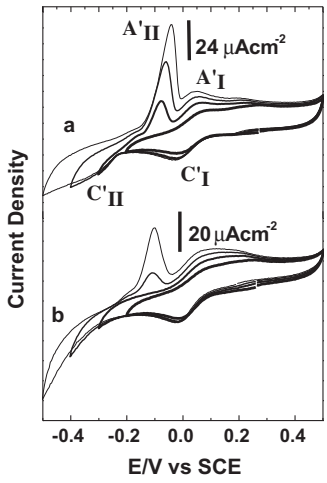

Fig. 9. Cyclic volatmmetry of ME/Cu-ZSM5 at different switching potential in (a) 0.1 M $NaNO_3$, (b) 0.05 M Na_2SO_4.

based-solutions, and (ii) the reduction of species Cu^{2+} at different sites of the zeolite framework; see next section.

3.5.4. Switching potential effect in presence of NO_3^- and SO_4^{2-}

To discriminate the hypothesis proposed in the previous section, experiments varying the cathodic potential limit were carried out on ME/Cu-ZSM5, Fig. 9. The scan was initiated from the open-circuit potential (E_{OCP}) in the negative direction and inverted at different potentials (E_λ). At $E_\lambda = -0.2$ V/SCE the characteristic behavior associated to redox process C_I'/A_I' are observed in all cases. At $E_\lambda = -0.3$ V/SCE an anodic peak (A_II' at c.a. −0.07 V/SCE) is only observed in presence of nitrate ions. Up to $E_\lambda = -0.3$ V/SCE an important increase in the current intensity is evident at peaks A_I' and A_II', associated to copper amount involved in faradic process. In addition, it is clear that the process A_II' is independent of the process C_I'.

These results put in evidence that in C_I' the formation of metallic copper is not achieved, it takes place when the E_λ increases up to −0.3 V/SCE, confirming the stabilization of Cu^+-ions at the interface of ME/Cu-ZSM5.

3.5.5. Voltammetry response of ME/H-ZSM5 in copper solutions

Fig. 10 exhibited the *i-E* characteristics obtained at different switching potential for ME/H-ZSM5 in $Cu(NO_3)_2$ 0.001 M + $NaNO_3$ 0.1 M (plot a) and $CuSO_4$ 0.0005 M + Na_2SO_4 0.05 M (plot b) solutions. These *i-E* characteristics permit to observe the existence of two cathodic peaks (C_I' and C_II'). The faradic process C_II' appears up to $E_\lambda = -0.2$ V/SCE. On the other hand, it can be observed the cross potential ($E_{cr} = -0.16$ V/SCE) and the nucleation potential ($E_n = -0.23$ V/SCE) discussed before. This electrochemical performance indicates that when the copper is in solution, the redox process is carried out in the uncovered part of glassy carbon. At $E_\lambda = -0.2$ V/SCE the magnitude of peaks C_I' and A_I' is important, with a small peak at c.a −0.045 V and −0.051 V/SCE in nitrate and sulfate solutions, respectively. These peaks are associated to process A_II' which increase when the E_λ is more negative, and shift to more positive potential with respect to the electrolyte in turn: 0.012 V (in NO_3^-) and 0.035 V (in SO_4^{2-}). Moreover, the peak A_I' should be masked due to the intensity of peak A_II' and the shift potential.

The reduction of copper over glassy carbon in presences of nitrites and sulfates was carried out using the same solutions as in Fig. 10. For curves b in Fig. 11, the profiles exhibit a cathodic peak C'' (at c.a. −0.15 V/SCE) and an anodic peak A'' (at c.a. 0.3 V/SCE), indicating that Cu^{2+} reduction occurs via a single two-electron step [50]. These electrochemical responses were compared with the cyclic voltammetry profiles in Fig. 10 at $E_\lambda = -0.5$ V/SCE (curves a, Fig. 11). The result obtained from Figs. 10 and 11, elucidate that the reduction of Cu^{2+} to Cu^0 at the interface of zeolite-modified electrodes (ME/H-ZSM5 and ME/Cu-ZSM5) take place via two one-electron steps through the Cu^+ stabilization, even at nitrate and sulfate based-solutions. In particular the stability at the interface of ME/H-ZSM5 when the copper is in solution suggest that reduction of Cu^{2+} to Cu^+ occurs in the external boundary of the zeolite.

3.5.6. Thermal treatment effect

With the aim to support the main goal in this work, which is to put in evidence the stabilization of the Cu^+ on the interface of zeolite modified electrode, multi-sweep cyclic voltammetry experiments, using different supporting electrolytes, were carried out on calcined (ME/Cu-ZSM5) and not calcined ($ME/Cu\text{-}ZSM5_{NC}$) ex-situ treated samples prior to electrode preparation. The results are reported in Fig. 12, in the case of not calcined sample (Fig. 12B) the current magnitude due to the copper ion interaction decreases as a result of the progressive depletion of electroactive species at the electrode surface, associated to ion exchange from bulk solution. Nevertheless, the inverse phenomenon can be observed at heat-treated Cu-zeolite material, Fig. 12A. This can be associated to progressive rehydration of the zeolite channels in

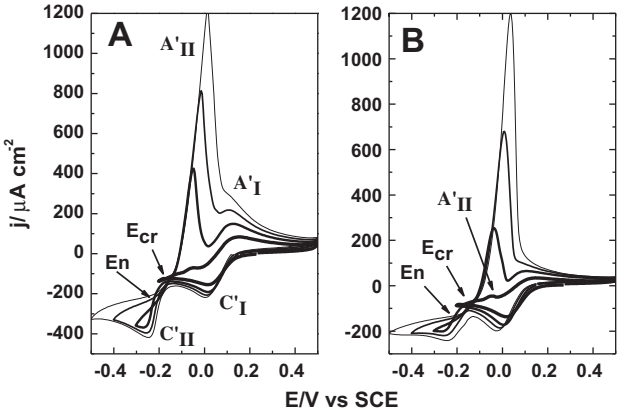

Fig. 10. Cyclic voltammetry of ME/H-ZSM5 at different switching potential in (a) $NaNO_3$ (0.1 M) + $Cu(NO_3)_2$ (0.001 M), (b) Na_2SO_4 (0.05 M) + $CuSO_4$ (0.0005 M). Scan rate of 20 mV/s.

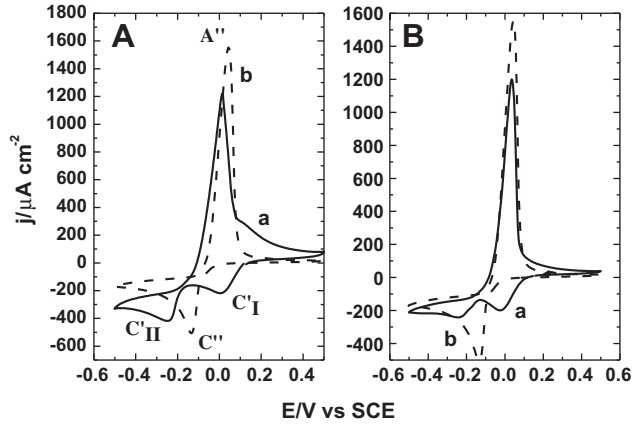

Fig. 11. Cyclic voltammetry of (a) UGC *y* (b) ME/H-ZSM5 in a solution of (A) $NaNO_3$ 0.1 M + $Cu(NO_3)_2$ 0.001 M and (B) Na_2SO_4 0.5 M + $CuSO_4$ 0.0005 M. Scan rate of 20 mV/s.

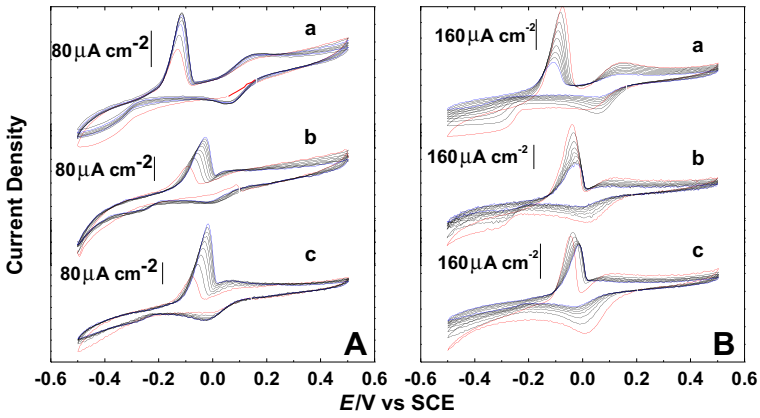

Fig. 12. Multi sweep cyclic voltammetry of ME/Cu-ZSM5 (A) Calcined, (B) Not calcined; in 0.1 M solutions (a) NaCl, (b) $NaNO_3$, (c) 0.05 M Na_2SO_4. Red line: first cycle. Blue line: last cycle. Scan rate of 20 mV s^{-1}.

contact with the solution. This fact promotes such an increment in current magnitude. However the ex-situ thermal treatment effects have not an important influence over stability of Cu^+.

3.5.7. Influence of electrode preparation

In order to discard possible effects in the redox reactions with respect to the solvent employed, experiments using acetone in the preparation of ZME were carried out. The sample was prepared as follow: 7 mg of PMMA were dissolved in 1 mL of acetone and mixed with 0.2 g of Cu-ZSM5 (ME/Cu-$ZSM5_{Ac}$). The electrochemical response was studied at different supporting electrolytes (Fig. 13). The results are compared with the electrochemical profiles in Fig. 9 at E_λ = −0.5 V/SCE. It can be observed that Cu^{2+} reduction at chloride-based solution occurs via two steps as was discussed before (curve a). On the other hand, it is possible to observe two peaks between −0.05 and −0.35 V/SCE and only one oxidation peak near to 0.02 V/SCE. Then, the redox process of copper occurs by one-step pathway with two electrons transferred. From the results in Fig. 13, one possible explanation is associated to the stability of the redox couple Cu^{2+}/Cu^+ in the ME/Cu-ZSM5 due to the π-back donation of d electrons of Cu^+ to π^*-antibonding orbital of double bond present in the methyl acrylate (MA) [27,28]. This π-back donation take place also in the double bond C = O as this functional group is found at acetone and MA structures. This Cu^+ electron-donation is due to the partial neutralization of cation-positive charge by oxygen in the framework. Thus, the zeolite structure also promotes the electrochemical stability. The cation charge decreased from +1 to +0.32, and HOMO energy increases from −14.115 eV (for free ion) to −5.170 or −5.317 eV (depending on cluster geometry) [51]. However, in the *i-E* characteristic, this interaction has not effect on the copper-electroreduction mechanism. At this conditions, the double bond C = C acquires a negative charge, whereas Cu^+ ion become more positive. Part of the charge transmitted to the molecule came from Cu^+ itself and other part from the zeolite framework, which acted as "electron reservoir" [52]. Even as in presence of double bond C = O this molecule received positive charge when interacting with zeolitic Cu^+. In these cases, the charge was transmitted from the molecule via Cu^+ to the zeolite framework. The electric charge on the cation did not change and zeolite framework acted again as "electron reservoir" but in this case the framework received the electrons.

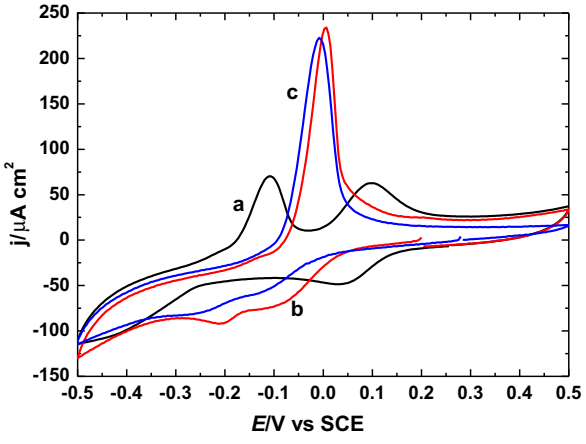

Fig. 13. *i-E* characteristics of ME/Cu-$ZSM5_{Ac}$ in 0.1 N (a) NaCl, (b) $NaNO_3$, (c) Na_2SO_4. The modified electrode was prepared using PMMA/Acetone.

4. Conclusions

In this work, a systematic study in order to understand the behavior of copper ions into the zeolite structure was carried out. For such an approach, structural, physicochemical and electrochemical techniques were employed. The preparation of zeolite-modified electrode (ME/Cu-ZSM5) deposited at a glassy carbon surface has been compared with its counterpart free of copper (ME/H-ZSM5). From a fundamental point of view, it has been established that (i) the *i-E* characteristic obtained by cyclic voltammetry at ME/Cu-ZSM5 represent a typical process corresponding to the redox-couple reaction Cu^{2+}/Cu^0 in two steps due to the stability of Cu^+ at the interface zeolite/substrate, even at nitrate and sulfate based-solutions; this phenomenon could be linked to some interactions of Cu^+ and the C = C bond containing in the organic solvent used and with the zeolite framework acting as an "electron reservoir", (ii) the incorporation of copper did not modify the zeolite structure, and (iii) the EPR spectra showed only isolated Cu^{2+} specie at ZSM5 structure. Then, this redox process takes place in the contact area through surface mediated electron-transfer process to electroactive species situated at the outer surface of the zeolite particles (i.e., those easily accessible to the electrons) [53]. Whereas the charge compensation is ensured by the electrolyte cation, followed by electron hopping to the probes located in the bulk of the solid, with concomitant migration of the electrolyte cation inside the zeolite structure.

Acknowledgments

The authors thank the financial support giving through the projects SIP-IPN 20110655, 20120499, ICyTDF PICS 09-321, and CONACYT 101319. M.A.O-T gratefully acknowledges the CONACyT (Mexico) for scholarship.

References

[1] D.R. Rolison, The intersection of electrochemistry with zeolite science, Stud. Surf, Sci. Catal. 85 (1994) 543–586.
[2] C. Senaratne, J. Zhang, M.D. Baker, C.A. Bessel, D.R. Rolison, Zeolite-modified electrodes: intra-versus extra zeolite electron transfer, J. Phys. Chem. 100 (1996) 5849–5862.
[3] E. Briot, F. Bedioui, K.J. Balkus, Electrochemistry of zeolite-encapsulated complexes: new observations, J. Electroanal. Chem. 454 (1998) 83–89.
[4] C.A. Bessel, D.R. Rolison, Topological redox isomers: surface chemistry of zeolite-encapsulated Co(salen) and $[Fe(bpy)3]^{2+}$ complexes, J. Phys. Chem. B. 101 (1997) 1148–1157.
[5] K.J. Balkus, A.K. Khanmamedova, K.M. Dixon, F. Bedioui, Oxidations catalyzed by zeolite ship-in-a-bottle complexes, Appl. Catal. A. 143 (1996) 159–173.
[6] C.A. Bessel, D.R. Rolison, Electrocatalytic reactivity of zeolite-encapsulated Co(salen) with benzyl chloride, J. Am. Chem. Soc. 119 (1997) 12673–12674.
[7] A.M. Mazloum, Z. Akrami, H. Kazemian, H.R. Zare, Electrocatalytic characteristics of uric acid oxidation at graphite–zeolite-modified electrode doped with iron (III), J. Electroanal. Chem. 586 (2006) 31–38.
[8] T. Rohani, M.A. Taher, A new method for electrocatalytic oxidation of ascorbic acid at the Cu(II) zeolite-modified electrode, Talanta 78 (2009) 743–747.
[9] O. Reza, R. Jahan-Bakhsh, F. Shahla, S. Alami-Valikchali, Electrochemical behavior of Ni(II) incorporated in zeolite y-modified carbon electrode: application for electrocatalytic oxidation of methanol in alkaline solution, J. Solid State Electrochem. 15 (2011) 1935–1941.
[10] A. Walcarius, L. Lamberts, E.G. Derouane, The methyl viologen incorporated zeolite modified carbon paste electrode-part 1. Electrochemical behavior in aqueous media. Effects of supporting electrolyte and immersion time, Electrochim. Acta. 38 (1993) 2257–2266.
[11] A. Walcarius, S. Rozanska, J. Bessiere, J. Wang, Screen-printed zeolite-modified carbon electrodes, Analyst 124 (1999) 1185–1190.
[12] T.W. Hui, M.D. Baker, Redox processes of methyl viologen cation radicals at zeolite y-modified electrodes, J. Phys. Chem. B. 106 (2002) 827–832.
[13] M.A. Zanjanch, S. Sohrabnezha, M. Arvand, M.F. Mousavi, Electrochemical study of the thionine dye incorporated into ZSM-5 and HZSM-5 zeolites, Russian J. Electrochem. 43 (2007) 758–763.
[14] J.B. Raoff, N. Azizi, R. Ojani, S. Ghodrati, M. Abrishamkar, F. Chekin, Synthesis of ZSM-5 zeolite: electrochemical behavior of carbon paste electrode modified with Ni (II) E-zeolite and its application for electrocatalytic oxidation of methanol, Int. J. Hydrogen Energy 36 (2011) 13295–13300.
[15] L. Čapek, V. Kreibich, J. Dědeček, T. Grygar, B. Wichterlová, Z. Sobalík, J.A. Martens, R. Brosius, V. Tokarová, Analysis of Fe species in zeolites by UV–VIS–NIR, IR spectra and voltammetry. Effect of preparation, Fe loading and zeolite type, Micropor. Mesopor. Mater. 80 (2005) 279–289.
[16] L. Smoláková, T. Grygar, L. Capek, O. Schneeweiss, R. Zboril, Speciation of Fe in Fe-modified zeolite catalysts, J. Electroanal. Chem. 647 (2010) 8–19.
[17] J. Pérez-Ramírez, F. Kapteijin, J.C. Groen, A. Doménech, G. Mul, J.A. Moulijn, Steam-activated FeMFI zeolites. Evolution of iron species and activity in direct N2O decomposition, J. Catal. 214 (2003) 33–45.
[18] H. Pang, J. Chen, L. Yang, B. Liu, X. Zhong, X. Wei, Ethanol electrooxidation on Pt/ZSM-5 zeolite-C catalyst, J. Solid State Electrochem. 12 (2008) 237–243.
[19] R. Singh, P.K. Dutta, MFI: a case study of zeolite synthesis, in: S.M. Auerbach, K.A. Carrado, P.K. Dutta (Eds.), Handbook of Zeolite Science and Technology, Marcel Dekker Inc, New York, 2003.
[20] C.D. Chang, A.J. Silvestri, The conversion of methanol and other O-compounds to hydrocarbons over zeolite catalysts, J. Catal. 47 (1997) 249–259.
[21] M.H. Groothaert, J.A. van Bokhoven, A.A. Battiston, B.M. Weckhuysen, R.A. Schoonheydt, Bis(μ-oxo) dicopper in Cu-ZSM-5 and its role in the decomposition of NO: a combined in situ XAFS, UV−Vis−Near-IR, and kinetic study, J. Am. Chem. Soc. 125 (2003) 7629–7640.
[22] B. Moden, P. Da Costa, B. Fonfe, D.K. Lee, E. Iglesia, Kinetics and mechanism of steady-state catalytic NO decomposition reactions on Cu–ZSM5, J. Catal. 209 (2002) 75–86.
[23] A. Kubacka, Z. Wang, B. Sulikowski, V.C. Corberan, Hydroxylation/oxidation of benzene over Cu-ZSM-5 systems: optimization of the one-step route to phenol, J. Catal. 250 (2007) 184–189.
[24] Y. Shibata, R. Hamada, T. Ueda, Y. Ichihashi, S. Nishiyama, S. Tsuruya, Gas-phase catalytic oxidation of benzene to phenol over Cu-impregnated HZSM-5 catalysts, Ind. Eng. Chem. Res. 44 (2005) 8765–8772.
[25] M.H. Groothaert, P.J. Smeets, B.F. Sels, P.A. Jacobs, R.A. Schoonheydt, Selective oxidation of methane by the bis(μ-oxo) dicopper core stabilized on ZSM-5 and mordenite zeolites, J. Am. Chem. Soc. 127 (2005) 1394–1395.
[26] J. Datka, E. Kukulska-Zajac, P. Kozyra, IR and TPD studies of the interaction of alkenes with Cu^+ sites in CuNaY and CuNaX zeolites of various Cu content. The heterogeneity of Cu^+ sites, J. Mol. Struc. 794 (2006) 261–264.
[27] E. Broclawik, P. Kozyra, J. Datka, IR studies and DFT quantum chemical calculations concerning interaction of some organic molecules with Cu^+ sites in zeolites, C. R. Chim. 8 (2005) 491–508.
[28] M.D. Baker, C. Senaratne, J. Zhang, Effects of supporting electrolyte and zeolite co-cations on the electrochemical response of zeolite modified electrode, J. Chem. Soc. Faraday. Trans. 88 (1992) 3187–3192.
[29] J.W. Li, G. Calzaferri, Copper-zeolite-modified electrodes: an intrazeolite ion transport mechanism, J. Electroanal. Chem. 377 (1994) 163–175.
[30] C. Nila, I. González, Thermodynamics of $Cu–H_2SO_4–Cl^-–H_2O$ and $Cu–NH_4Cl–H_2O$ based on predominance-existence diagrams and pourbaix-type diagrams, Hidrometallurgy 42 (1996) 63–82.
[31] S. Senthilkumar, R. Saraswathi, A novel zeolite-multiwalled carbon nanotube composite for the electroanalysis of copper(II) ion, J. Appl. Electrochem. 41 (2011) 909–917.
[32] P. Joo-Hyoung, P. Hye Jun, B. Joon Hyun, N. In-Sik, S. Chae-Ho, L. Jong-Hwan, C. Byong, H. Se, Hydrothermal stability of CuZSM5 catalyst in reducing NO by NH_3 for the urea selective catalytic reduction process, J. Catal. 240 (2006) 47–57.
[33] Y. Zhang, I.J. Drake, A.T. Bell, Characterization of Cu–ZSM-5 prepared by solid-state ion exchange of H–ZSM-5 with CuCl, Chem. Mater. 18 (2006) 2347–2356.
[34] O.P. Tkachenko, K.V. Klementiev, M.W.E. van den Berg, N. Koc, M. Bandyopadhyay, A. Birkner, C. Woll, H. Gies, Reduction of copper in porous matrixes. stepwise and autocatalytic reduction routes, J. Phys. Chem. B. 109 (2005) 20979–20988.
[35] A. Ibraheem-Othman, Preparation and characterization of copper nanoparticles encapsulated inside ZSM-5 zeolite and NO adsorption, Mater. Sci. Eng. 459 (2007) 294–302.
[36] M.A. Ali, B. Brisdon, W.J. Thomas, Synthesis, characterization and catalytic activity of ZSM-5 zeolites having variable silicon-to-aluminum ratios, identification of ZSM-type and other 5-ring containing zeolites by i.r. spectroscopy, Appl. Catal. A 252 (2003) 149–162.
[37] L.M. Parker, D.M. Bibby, An infrared study of H_2O and D_2O on HZSM-5 and DZSM-5, Zeolites 13 (1993) 107–112.
[38] E.S. Rufino, E.E.C. Monteíro, Infrared study on methyl methacrylate–methacrylic acid copolymers and their sodium salts, Polymer 44 (2003) 7189–7198.
[39] P.J. Carl, S.C. Larsen, EPR Study of copper-exchanged zeolites: effects of correlated g- and A-strain, Si/Al ratio, and parent zeolite, J. Phys. Chem. B. 104 (2000) 6568–6575.
[40] R.S. Drago, Physical methods in chemistry, W. B. Saunders, Philadelphia, 1992.
[41] V.F. Anufrienko, S.A. Yashnik, N.N. Bulgakov, T.V. Larina, N.T. Vasenin, Z.R. Ismagilov, A study of linear copper oxide structures in the channels of the ZSM-5 zeolite by electronic diffuse reflectance spectroscopy, Phys. Chem. 392 (2003) 207–211.
[42] O.P. Krivoruchko, N.T. Vasenin, T.V. Larina, V.F. Anufrienko, V.N. Parmon, Detection of uncommon ordering of Cu^{2+} ions in the zeolite Cu(n)ZSM-5 pore space by EPR and electronic diffuse reflectance spectroscopy, Phys. Chem. 430 (2010) 13–16.
[43] M.A. Oliver-Tolentino, A. Guzmán-Vargas, E.M. Arce-Estrada, A. Manzo-Robledo, Electrochemical behavior of glassy carbon electrode modified with copper-ZSM5, ECS Trans. 29 (2010) 399–408.
[44] J. Vazquez-Arenas, I. Lazaro, R. Cruz, Electrochemical study of binary and ternary copper complexes in ammonia-chloride medium, Electrochim. Acta 52 (2007) 6106–6117.
[45] N. El Murr, M. Kerkeni, A. Sellami, Y. Ben Taarit, The zeolite-modified carbon paste electrode, J. Electroanal. Chem. 246 (1988) 461–465.
[46] R.M. Barrer, A.J. Walker, Imbibition of electrolytes by porous crystals, Trans. Faraday. Soc. 60 (1964) 171–184.
[47] B.R. Shaw, K.E. Creasy, C.J. Lanczycki, J.A. Sargeant, M. Tirhado, Voltammetric response of zeolite-modified electrodes, J. Electrochem. Soc. 135 (1988) 869–876.
[48] J. Reiter, J. Vondrák, Z. Micka, The electrochemical redox processes in PMMA gel electrolytes-behaviour of transition metal complexes, Electrochim Acta 50 (2005) 4469–4476.
[49] K. Hu, D. Lan, X. Li, S. Zhang, Electrochemical DNA biosensors on nanoporous gold electrode and multifunctional encode DNA-Au bio bar codes, Anal. Chem. 80 (2008) 9124–9130.
[50] J. Vazquez-Arenas, G. Vázquez, A.M. Meléndez, I. González, The effect of the Cu^{2+}/Cu^+ step on copper electrocrystallization in acid noncomplexing electrolytes, J. Electrochem. Soc. 154 (2007) 473–481.
[51] J. Datka, E. Kukulska-Zajac, P. Kozyra, IR studies and DFT calculations concerning the status of Cu^+ ions in CuZSM-5 and CuMCM-41, Catal. Today 90 (2004) 109–114.
[52] A. Goursot, B. Coq, F. Fajula, Toward a molecular description of heterogeneous catalysis: transition metal ions in zeolites, J. Catal. 216 (2003) 324–332.
[53] P.K. Dutta, M. Ledney, Charge-transfer processes in zeolites: toward better artificial photosynthetic models, Progr. Inorg. Chem. 44 (1997) 209–271.